The Mechanical Structures of Bamboos in Viewpoint of Functionally Gradient and Composite Materials

SHIGEYASU AMADA, TAMOTSU MUNEKATA, YUKITO NAGASE,
YOSHINOBU ICHIKAWA, ATSUSHI KIRIGAI AND YANG ZHIFEI
Department of Mechanical Engineering
School of Engineering
Gunma University
1-5-1 Tenjin, Kiryu, Gunma 376
Japan

(Received August 20, 1994)
(Revised April 6, 1995)

ABSTRACT: The structures of bamboos have been adapted to our natural environment over a long period of time. They are a composite material reinforced axially by fibers called bundle sheath. Furthermore, they have a hierarchical gradient structure, that is, a macroscopic gradient structure in culm (corresponding to trunk of wood) diameter, culm thickness and node length, and a microscopic one in the bundle sheath distribution. The macroscopic gradient structure leads to a constant surface stress at every height and the microscopic gradient structure provides a strength distribution in radial direction adapting to bending stress due to wind loads.

KEY WORDS: bamboo, functionally gradient materials (FGM), hierarchy, smart structure, adapting structure.

1. INTRODUCTION

FOR A LONG time the structures of plants have been adapted to our natural environment. Of all those plants bamboo can be a typical one. Bamboos have far superior characteristics than newly developing materials. It must be said that bamboo is a good and smart model of the advanced materials. Looking at the cross section of the bamboo culm (trunk), as shown in Figure 1(a), the distributed solid dots are recognized. These are called bundle sheath which plays a role of fibers in composite materials. The distributed structure of bundle sheaths corresponds to the one of functionally gradient materials [1] developed recently. The culm is composed of exodermis (bark), vascular bundle sheaths, parenchymatous cells (soft tissue cells) and endodermis (inner surface layer), as shown in Figure 1(b). A vascular bundle is made up of two kinds of tube, sieve tube (transporting nutrition) and vessel (transporting water).

0021-9983/96/07 800-20 $10.00/0

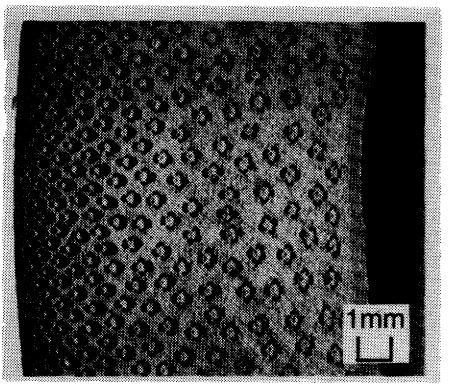

(a)

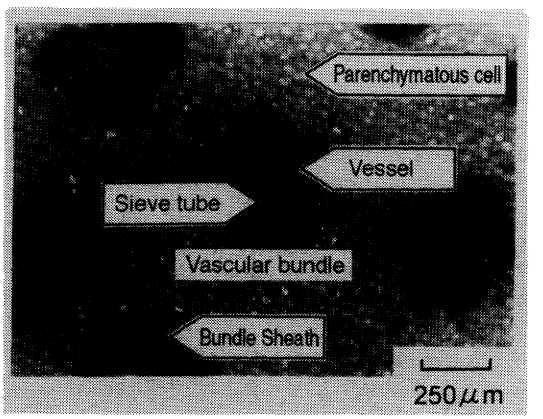

(b)

Figure 1. *Picture of cross-section of bamboo: (a) cross section; (b) vascular bundle sheath.*

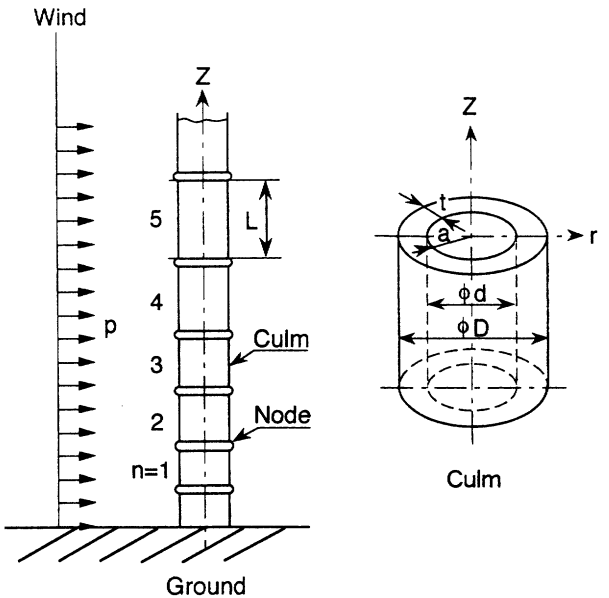

Figure 2. *Configuration and notations.*

A bamboo has three main characteristics of the structure different from other plants. First, the bamboos have many nodes (circular disc discretely inserted into the hollow culm), as shown in Figure 2, which may play a role of the axial crack arrester and a function to prevent a bending buckling. In the second, the culm thickness, outer diameter and node distance change regularly with respect to height from the ground. We can call these characteristics the macroscopic, functionally gradient structure. In the third, the volume fraction of bundle sheaths increases from the inner to outer surface of the culm. It may be called by the microscopic, functionally gradient structure.

There have been a few studies about bamboo. Oda studied the bamboo structure based on an optimum design [2,3]. Nokata [4] and Chujou [5] measured the strength and Young's modulus distributions in the cross section. We studied bamboos based on composite and functionally gradient structural materials, and presented several results [6–8].

This paper presents the mechanical structure of bamboos and clarifies the relations between their strength and gradient structure based on composite, functionally gradient and hierarchical structural materials.

2. MATERIALS AND METHODS

Bamboo used in this experiment is Mousou-bamboo (*Phyllostachys edulis Riv.*). Typical chemical constituents of bamboo culm are listed in Table 1 [9].

Table 1. Chemical constituents of bamboo culm (in percent).

Cellulose	Lignin	Soluble Matters	Nitrogen	Ash
44.51	20.54	32.24	0.27	2.44

Since bamboo ceases to grow after one year, we cut one of two years old-bamboos out of the forest. All the experiments were done within two months after cut.

1. Diameter and node length (length between the adjacent nodes) were experimentally measured with respect to coordinate as shown in Figure 2. Then the culm was divided into several cylinders and thickness of their cylinder walls were also experimentally measured.
2. Strength and Young's modulus in the axial direction, along the bundle sheaths, were measured by using tensile test as shown in Figure 3. The tensile specimens are sliced out of the bamboo culm at different heights, which is shown in Figure 4.
3. To obtain the circumferential properties of bamboo culm, the compression tests are carried out by using the ring specimens as shown in Figure 5. The specimens with 10 mm width are cut out of the bamboo culm at different heights.
4. Bulk density is measured with scales using the specimens, cube with 10 mm sides.

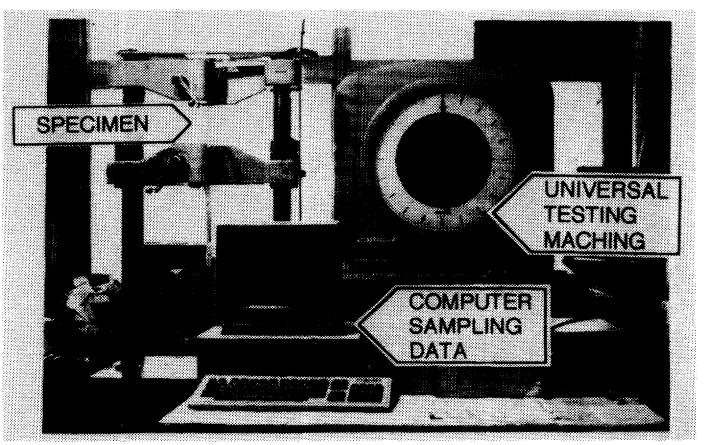

Figure 3. *System of tensile test.*

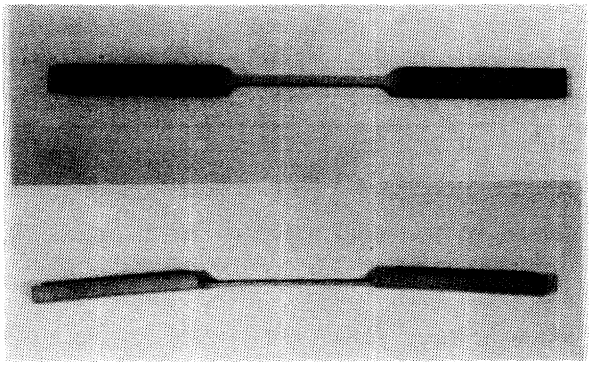

Figure 4. *Sliced tensile specimen.*

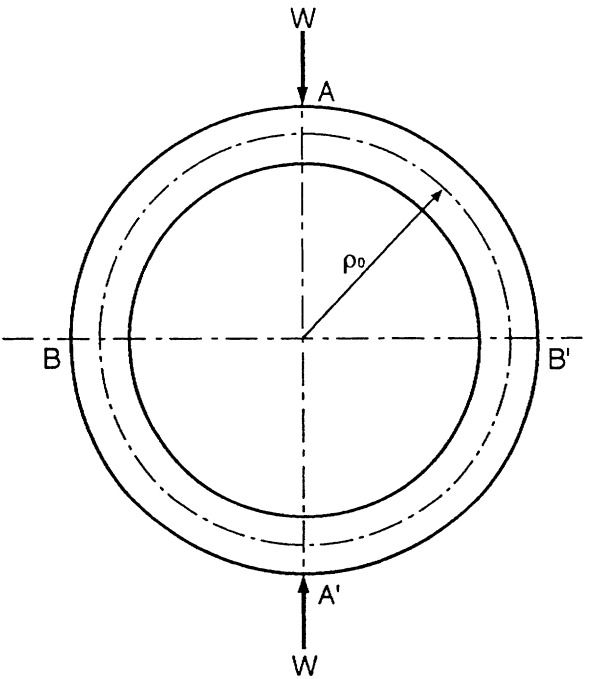

Figure 5. *Compression specimen of bamboo ring.*

3. SHAPES: MACROSCOPIC GRADIENT STRUCTURE

Figure 6 shows the distributions of diameter D, thickness t and node length L with respect to culm number n. L has the maximum value at the middle point of total height, which is almost the same place as the lowest branch. D and t decrease monotonically and almost linearly. These three properties form the gradient structure and can lead to the superior bending rigidity against the environmental loads. We call these structures by the macroscopic gradient structure compared with the microscopic one presented later.

The bamboos are mainly subjected to wind loads which can be assumed to be uniform over their entire length as shown in Figure 2. Moment in this case is given by

$$M = \frac{p}{2} \cdot (1 - z)^2 \tag{1}$$

Let the non-dimensional moment be defined by

$$\bar{M} = \frac{M}{M_{max}} \tag{2}$$

where M_{max} is moment at $z = 0$.

The section modulus Z_m of a hollow cylinder is given by

$$Z_m = \frac{\pi}{32} \cdot \frac{[D^4 - (D - 2t)^4]}{D} \tag{3}$$

Introducing the non-dimensional section modulus $\bar{Z}_m$, defined by

$$\bar{Z}_m = \frac{Z_m}{Z_{m,max}} \tag{4}$$

where $Z_{m,max}$ stands for the section modulus at $Z = 0$. Then, the non-dimensional stress on the culm surface due to bending moment is calculated from

$$\bar{\sigma}_B = \frac{\bar{M}}{\bar{Z}_m} \tag{5}$$

The obtained results of $\bar{M}$, $\bar{Z}_m$ and $\bar{\sigma}_B$ are shown in Figure 7. The results indicate that the maximum surface stress at every height is almost a constant except for the top region. Therefore, the bamboo can be classified macroscopically a smart structure based on an optimum design. This concept was proposed first by Metzer [10]. He got an excellent result for spruce in accordance with this hypothesis of constant mechanical stress along the length of the trunk.

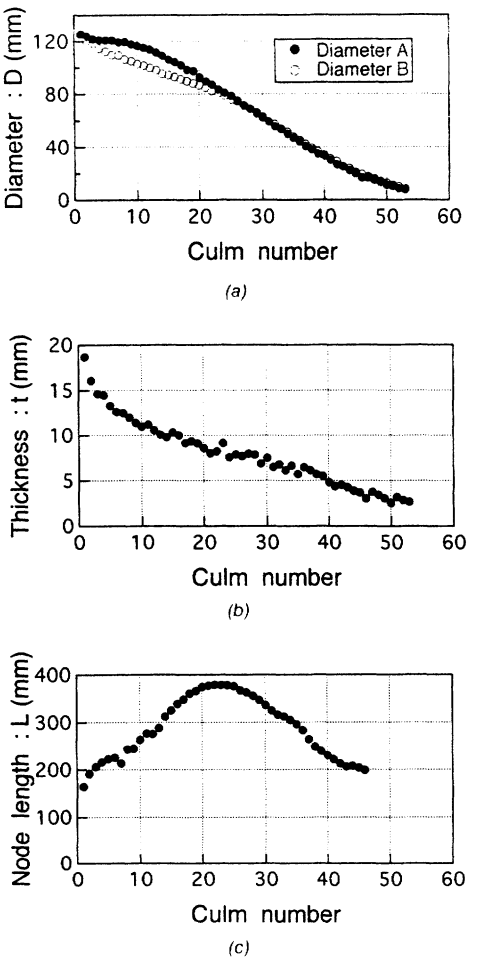

Figure 6. *Bamboo geometry: (a) diameter; (b) thickness; (c) culm number.*

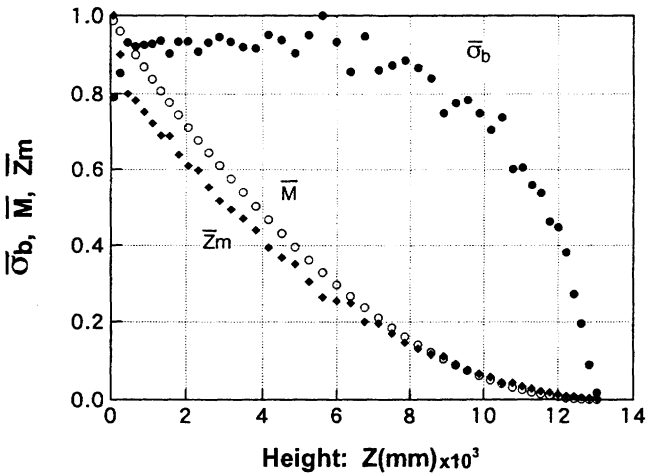

Figure 7. *Non-dimensional section modulus, moment and stress along height.*

4. FIBER REINFORCED CULM: MICROSCOPIC GRADIENT STRUCTURE

4.1 Image Analysis of Fiber Distribution

As mentioned in the introduction, the bamboo culm is a fiber reinforced composite. Although fibers and matrix consist of hollow cells, they are assumed to be solid ones as shown in Figure 1(a). Also, it is assumed that they are made from different materials. First, we measure the volume fraction of fibers by image analysis. The measuring system is given in Figure 8. The processing procedure is carried out as follows:

1. A cross section of the culm is imaged by CCD video camera. The picture image is painted by 484 × 252 dots on the display screen of a computer.
2. The data of the picture image is transformed into the binary-processed image as shown in Figure 9 to separate the bundle sheaths from the culm tissues (matrix).
3. By using the processed image, the volume fraction of fibers is measured by counting the dots painting the bundle sheaths.

4.2 Measured Results

The measured volume fractions of the bundle sheaths with respect to non-dimensional radius are shown in Figure 10. The highest value is about 60% in the outer layer and the lowest is around 15% in the inner layer. So that, in the outer region the fibers distribute in dense. This fiber distribution makes fit to the stress distribution due to bending moment, which will be discussed later in this paper.

The volume fraction of bundle sheath along the entire length is shown in Figure

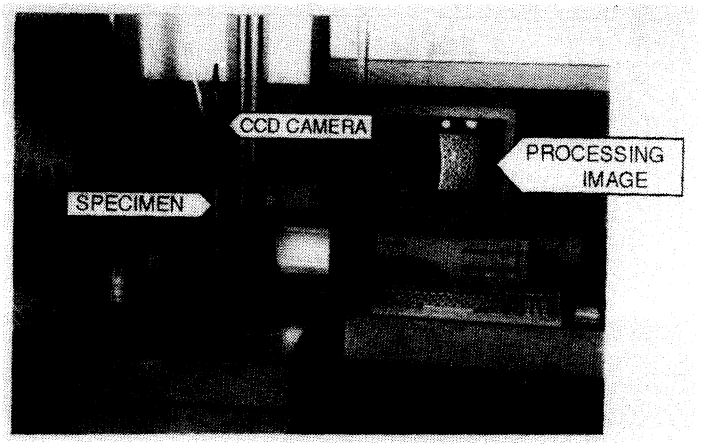

Figure 8. *System of image analysis for measuring fiber content.*

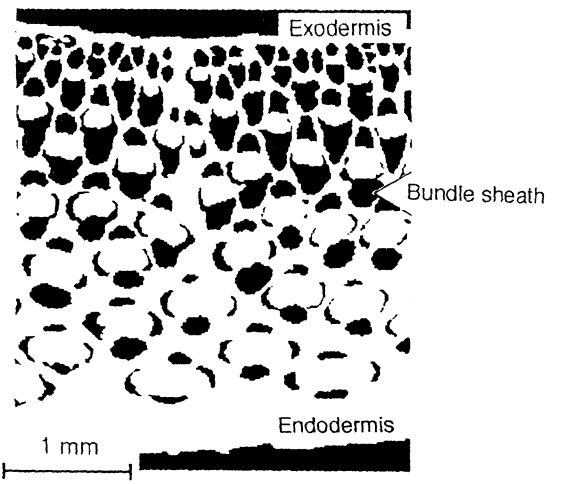

Figure 9. *Binary processed image of cross section.*

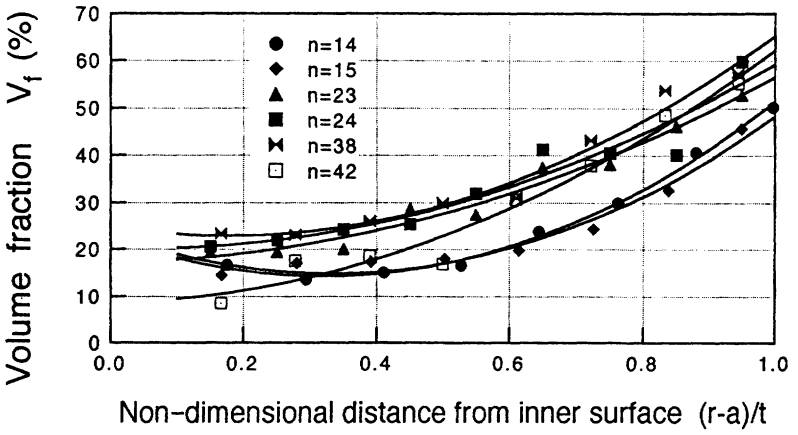

Figure 10. *Volume fraction of bundle sheath in non-dimensional radius.*

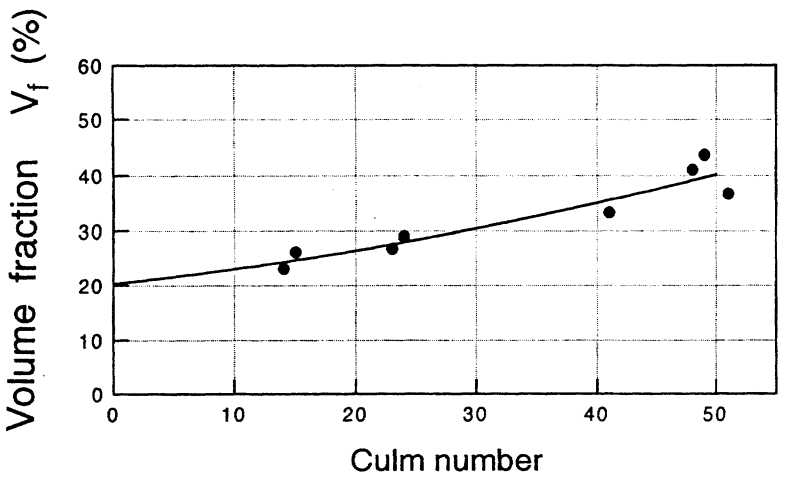

Figure 11. *Volume fraction of bundle sheath in axial direction.*

11. It increases linearly with height and has the maximum value at its top. Approaching to the bamboo top, diameter and thickness decrease, which deteriorates considerably the bending strength. The larger volume fraction in the top region is distributed to compensate this deterioration. This is the second useful aspect as a smart structure the bamboo possesses.

5. MATERIAL PROPERTIES

5.1 Axial Tensile Strength

The measured axial tensile strength of the sliced bamboo specimens is shown in Figure 12 with respect to the non-dimensional radius. It is lower in the inner region and increases parabolically with radius. This distribution pattern is the same as the one of the bending stress due to environmental loads. This is the third aspect which enables us to label as a smart structure. This will be discussed further in Section 7.

The measured tensile strength is plotted with respect to the volume fraction of the bundle sheaths as shown in Figure 13. We assume that matrix and fiber are made from different materials. If we use rule of mixture, the total axial strength σ_z is given by the strength σ_f and σ_m of the bundle sheaths and matrix, and by the volume fraction V_f of the bundle sheath,

$$\sigma_z = \sigma_f \cdot V_f + \sigma_m \cdot (1 - V_f) \tag{6}$$

and then we can draw a straight line through the average data in Figure 13. In Figure 13, the point where a straight line hits the vertical line at $V_f = 0(\%)$ in-

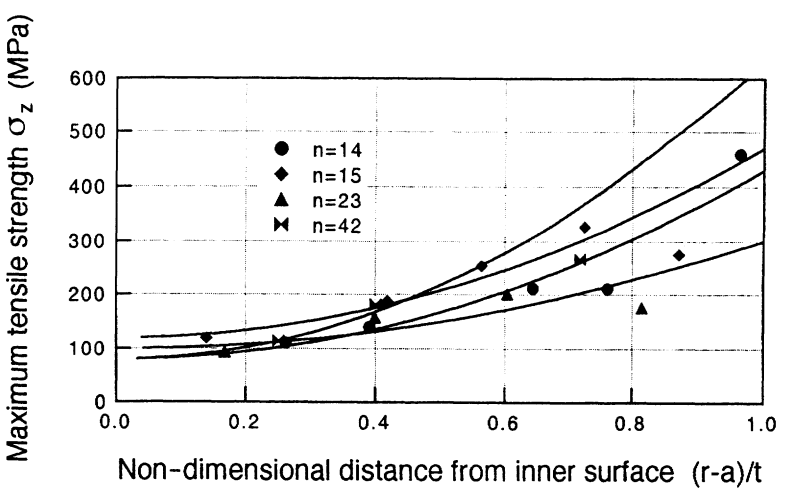

Figure 12. *Maximum tensile strength with respect to non-dimensional radius.*

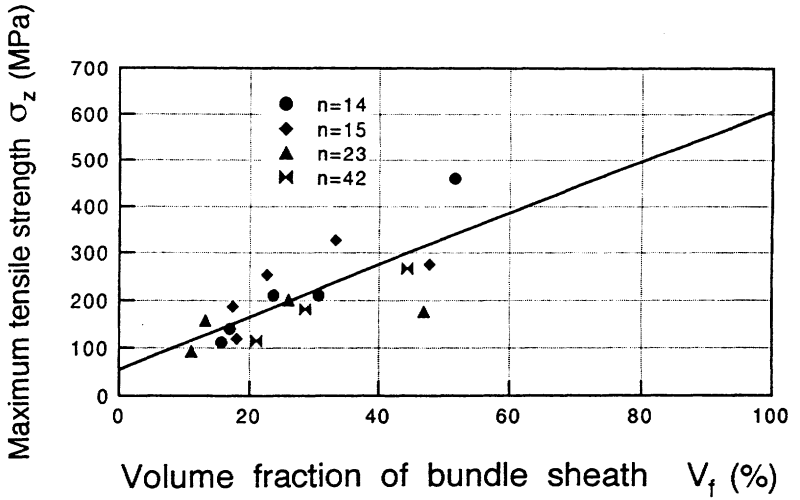

Figure 13. *Maximum tensile strength vs. volume fraction of bundle sheath.*

dicates the matrix strength and is 50 MPa. Value of the tensile strength at $V_f = 100(\%)$ corresponds to the bundle sheath strength which is 610 MPa. Therefore, tensile strength of the bundle sheath is more than 12 times larger than matrix strength.

5.2 Axial Elastic Modulus

The marvelous flexibility of the bamboos is mainly related to its Young's modulus. Figure 14 shows the distributions of the axial Young's modulus with respect to the non-dimensional radius. It can be inferred that the surface layer of the bamboo culms is more rigid than the inner layer. This characteristic allows it to adapt to the environmental loads.

The Young's modulus data are plotted with respect to V_f in Figure 15. Using rule of mixture, the axial Young's modulus E_z is given by

$$E_z = E_f \cdot V_f + E_m \cdot (1 - V_f) \tag{7}$$

where E_f and E_m are the Young's modulus of the bundle sheaths and matrix, respectively. Then, we can draw a line through the average dotted data in Figure 15. From this line, we can get the values $E_m = 2$ GPa and $E_f = 46$ GPa for matrix and bundle sheath, respectively.

5.3 Circumferential Strength and Elastic Modulus

Since the bundle sheath runs only in the axial direction, there are no reinforced effects for the circumferential properties. We measure these properties by the

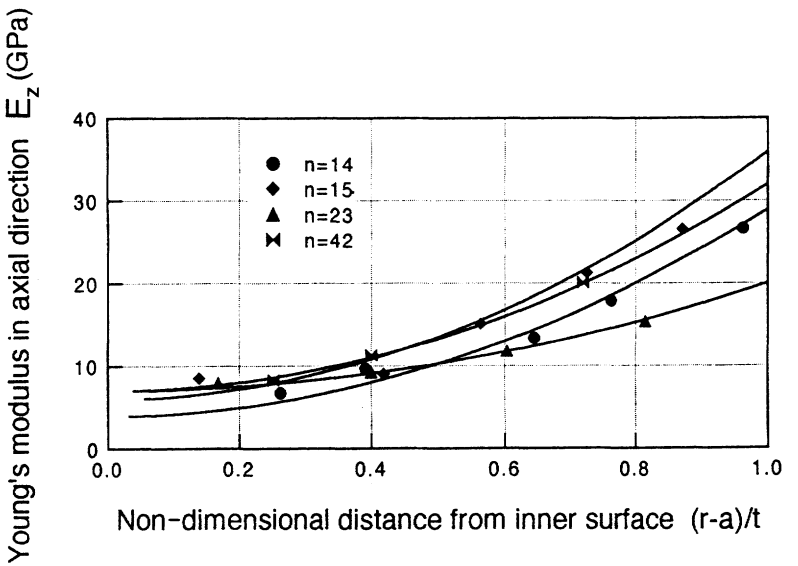

Figure 14. *Axial Young's modulus with respect to non-dimensional radius.*

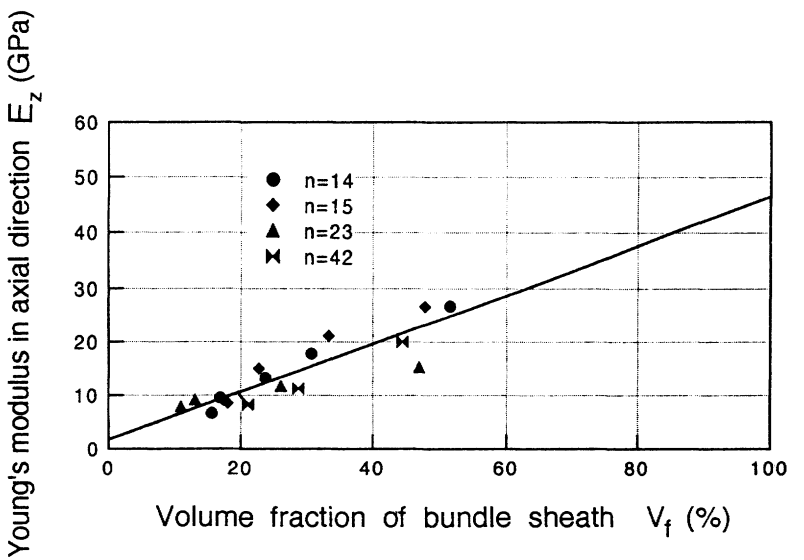

Figure 15. *Axial Young's modulus vs. volume fraction of bundle sheath.*

compression tests of the bamboo ring as mentioned in section 2. Applying curved beam analysis [11] to the ring specimen, the circumferential strength σ_θ and Young's modulus E_θ were evaluated from the following relations.

$$\sigma_\theta = \frac{W}{A\pi(1 + \varkappa)}\left[1 - \frac{t}{\varkappa(\varrho_o - t)}\right] \tag{8}$$

$$E_\theta = \frac{W\varrho_o}{\delta A}\left[\frac{1}{\varkappa}\left(\frac{\pi}{4} - \frac{2}{\pi}\right) - \frac{2}{\pi(1 + \varkappa)}\right] \tag{9}$$

where $\varkappa$ is section modulus of the ring specimen given by

$$\varkappa = \frac{1}{3}\left(\frac{t}{2\varrho_o}\right)^2 + \frac{1}{5}\left(\frac{t}{2\varrho_o}\right)^4 + \cdots \tag{10}$$

In Equations (8), (9) and (10), W and δ are compressive load and deflection at loading point, A is cross-sectional area and $\varrho_o = (D/2 - t/2)$ is radius of ring. Substituting the data of the compression test into Equations (8) and (9), we get the following values.

$$\sigma_\theta = 23 \text{ MPa}$$

$$E_\theta = 2.0 \text{ GPa}$$

The value of the circumferential strength is about a half of the axial matrix strength given in 5.1. Since a matrix composed of a hexagonal cylinder [12] has microscopically anisotropic characteristics, its lateral strength is weaker than the axial one, whereas the circumferential Young's modulus agrees completely with the axial one of matrix.

5.4 Density

The distributions of bulk density ϱ with respect to non-dimensional radius are shown in Figure 16. The values of bulk density are plotted with V_f as shown in Figure 17. Rule of mixture is assumed to be as follows:

$$\varrho = \varrho_f \cdot V_f + \varrho_m \cdot (1 - V_f) \tag{11}$$

where ϱ_f and ϱ_m are bulk density of the bundle sheath and matrix, respectively. Drawing a straight line through the average dots in Figure 17, we get the values of ϱ_f and ϱ_m, as

$$\varrho_f = 1.16 \text{ g/cm}^3$$

$$\varrho_m = 0.67 \text{ g/cm}^3$$

The bulk density of the bundle sheath is almost double of matrix.

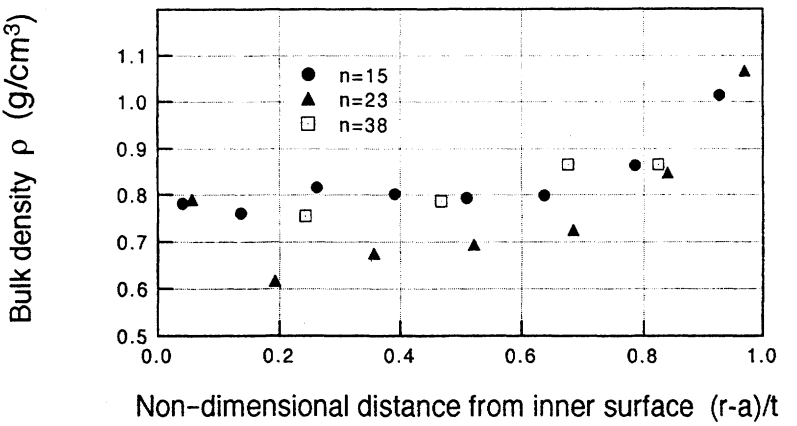

Figure 16. *Bulk density distribution with respect to non-dimensional radius.*

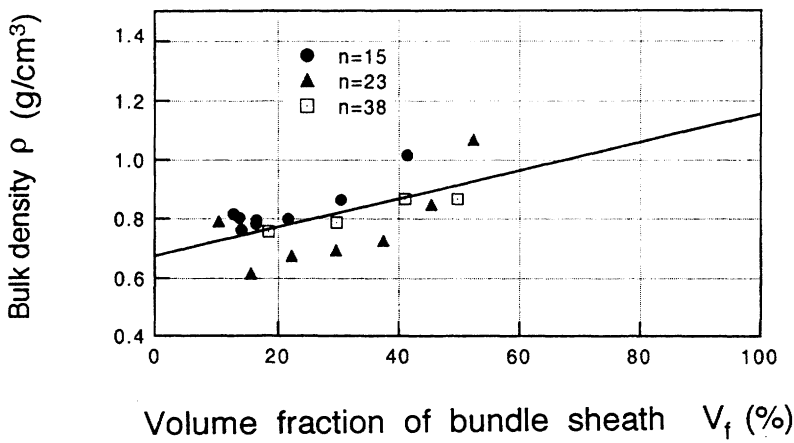

Figure 17. *Bulk density vs. volume fraction of bundle sheath.*

6. PREDICTION OF STRENGTH AND YOUNG'S MODULUS ALONG HEIGHT

We measured the axial tensile strength and Young's modulus of the specimens for several culm numbers. At the same time, the volume fractions of the bundle sheaths are evaluated by the image analysis. The cross section of the specimens is 4 mm in width and culm thickness t was shown in Figure 2.

The measured values are marked by solid dots in Figure 18. We have already had the strength and Young's modulus of the bundle sheath and matrix, respectively. Using these data, measured V_f and a rule of mixture given by Equations (6) and (7), these values can be calculated. The obtained results are shown in Figure 18. The theoretical predictions agree approximately with the measured data. This agreement verified applicability of a rule of mixture given in Equations (6) and (7).

7. DISCUSSION ON GRADIENT STRUCTURE OF BUNDLE SHEATH

As mentioned in 5.1, the tensile strength in the cross section of bamboo culm varies parabolically with respect to radius. We now discuss the origin of this probable smart gradient structure. The bamboo is subjected to the wind load which generates bending moment M. Applying a theory of composite cylindrical beams to the culm's cross section as shown in Figure 19, the culm can be modeled by a multi-layered cylinder. The stress σ_j in the jth layer is given by

$$\sigma_j = \frac{E_j \cdot R_j \cdot M}{\left\{\sum^{N} E_j \cdot I_j\right\}} \tag{12}$$

where E_j and I_j are the Young's modulus and moment of inertia of the jth layer. R_j is radius of the jth layer and N is number of the layers. Introducing $\sigma_{j,max}$, which corresponds to the surface-layer stress, defined by

$$\sigma_{j,max} = \sigma_j \cdot I_{j=N} = \frac{E_N \cdot R_N \cdot M}{\{\Sigma E_j \cdot I_j\}} \tag{13}$$

then the non-dimensional stress $\bar{\sigma}_j$ is defined by

$$\bar{\sigma}_j = \frac{\sigma_j}{\sigma_{j,max}} = \frac{E_j \cdot R_j}{E_N \cdot R_N} \tag{14}$$

This is essentially the generated stress under bending moment. Using the measured data E_j in Figure 14, Equation (14) is calculated and the results with respect to radius is shown by hollow dots of various shapes and solid lines for four different culm numbers in Figure 20.

The strength distributions with respect to radius were shown in Figure 12. Ex-

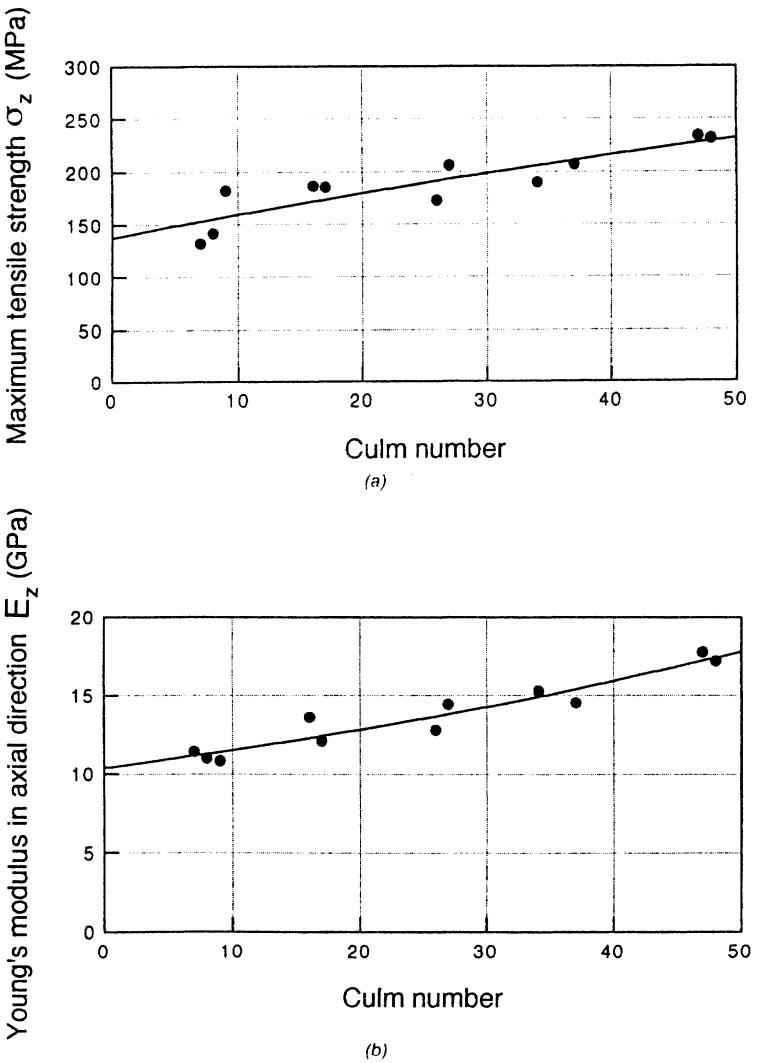

Figure 18. *Comparisons of theoretical strength and Young's modulus with measured ones: (a) tensile strength; (b) Young's modulus.*

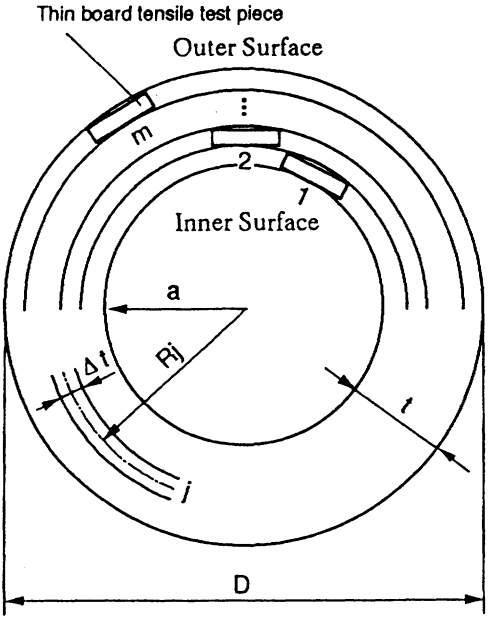

Figure 19. *Multi-layered cylindrical model.*

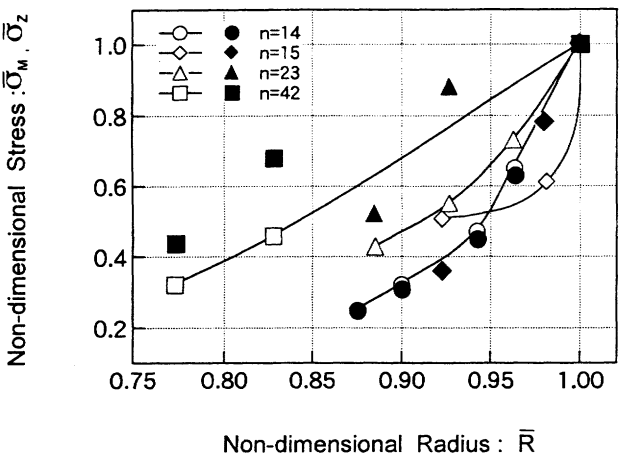

Figure 20. *Comparison of bending stress with strength distribution.*

pressing $\bar{\sigma}_z$ in non-dimensional form with $\sigma_{z,max}$ (σ_z at the most outer layer), the non-dimensional strength $\bar{\sigma}_z$ is given by

$$\bar{\sigma}_z = \frac{\sigma_z}{\sigma_{z,max}} \tag{15}$$

These values are marked by solid dots of various shapes in Figure 20. This distribution is provided by the bamboos to resist against the bending stress due to the environmental loads.

Taking into the consideration of the individual difference of the bamboos, these two kinds of the values calculated from Equations (14) and (15) are approximately close. In other words, the distributions of the bundle sheath adapt to the environmental loads. This is the third smart feature which the bamboos have acquired.

8. CONCLUSIONS

The bamboos have a typical structure of composite material reinforced axially by fibers called bundle sheath. The entire shapes and the bundle sheath distributions leads to wonderful characteristics. Focusing on the mechanical structures of the bamboos, we concluded the following points.

1. The bamboos have a hierarchical gradient structure, that is, a macroscopic gradient structure in culm diameter, thickness and node distance, and a microscopic one in the bundle sheath distribution.
2. The strength of bundle sheaths is about 12 times higher than the matrix one. The Young's modulus of bundle sheaths is about 23 times as high as the one of matrix. These data are listed in Table 2 as compared with several woods [13].

Table 2. Mechanical properties of several woods and bamboo.

Woods	Strength σ_f (MPa)	Young's Modulus E (GPa)	Density ϱ (g/cm^3)
Cedar	29.3–48.5	4.4–9.8	0.29–0.46
Fir	30.7–33.8	5.9–6.7	0.31–0.34
Pine	34.0–41.6	6.5–8.8	0.35–0.42
Spruce	31–40	7.3–8.5	0.38
Hickory	62.5–81.0	8.9–11.4	0.56–0.67
Oak	47.7–74.9	7.9–12.4	0.53–0.61
Bamboo (Fiber)	610	46	1.16
Bamboo (Matrix)	50	2	0.67
Bamboo (Composite)	140–230	11–17	0.6–1.1

3. The bamboos have a smart adapted structure to the environmental loads and their characteristics are given by the following items:
   (a) The maximum surface stress at every height is almost a constant along the entire length under the environmental loads, that is, wind.
   (b) The volume fraction of the bundle sheath increases linearly with height to compensate for a decrease of stiffness due to the decrease of culm diameter and thickness.
   (c) The distribution of the bundle sheath with respect to radius approximately fits the bending stress due to the wind loads.

The functionally gradient materials have not yet acquired a hierarchical structure. Marvelously the bamboos have done it. It will be very helpful to refer these smart ideas for the development of new functional materials.

REFERENCES

1. Rabin, B. H. and I. Shiota. 1995. *MRS Bulletin*, 20:14–18.
2. Oda, J. 1980. *Trans. Japan Soc. Mech. Engr.*, Ser. A, 46:997–1002.
3. Oda, J. 1985. *J. Trans. ASME*, Ser. R, 107:88–93.
4. Nokata, F. and K. Seo. 1990. *FGM News*, The Soc. of Non-Traditional Tech., Japan, 8:1–2.
5. Chuujou, S., et al. 1990. *Zairyou, Japanese Soc. of Materials Eng.*, pp. 847–851.
6. Amada, S., et al. 1992. *Procd. the 5th Symp. Functionally Gradient Struct.*, The Soc. of Non-Traditional Technology, Japan, pp. 293–297.
7. Amada, S., et al. 1993. *Procd. the 5th Bio-engr. Div. Conf. of JSME*, Japanese Soc. Mech. Engrs., pp. 62–64.
8. Amada, S., et al. 1993. *Procd. the 5th Bio-engr. Div. Conf. of JSME*, Japanese Soc. Mech. Engrs., pp. 59–61.
9. Shibamoto, T., et al. 1954. *Enshuu-rin Report, Univ. of Tokyo*, 47:204–207.
10. Metzger, K. 1983. *Mundener Forstliche Hefte*, 3 Heft, pp. 188–205.
11. Wempner, G. 1973. *Mechanics of Solids*, McGraw-Hill, p. 362.
12. Gibson, L. J. and M. F. Ashby. 1988. *Cellular Solids*, Pergamon Press, p. 278.
13. Bodig, J. and Jayne, B. A. 1993. *Mechanics of Wood and Wood Composites*, Kriger Publishing Co., pp. 666–671.